Qi *et al. Journal of Ovarian Research* (2025) 18:81
https://doi.org/10.1186/s13048-025-01659-6

Journal of Ovarian Research

RESEARCH Open Access

NCAPH promotes glucose metabolism reprogramming and cell stemness in ovarian cancer cells through the MEK/ERK/PD-L1 pathway

Yingying Qi[1†], Aiping Wang[1†], Silin Chen[1†] and Wei Chen[1*]

Abstract

Backgrounds Ovarian cancer is a prevalent malignant tumor that affects the female reproductive system with the characteristic of high heterogeneity. Non-structural maintenance of chromosomes condensin I complex subunit H (NCAPH) has been implicated in a variety of cancers.

Methods The expression of NCAPH before and after transfection were assessed using RT-qPCR and western blot analysis. Cell stemness was evaluated through spheroid formation assay. The extracellular acidification rate (ECAR) of ovarian cancer cells was measured utilizing Seahorse Glycolysis Stress Test Assay while oxygen consumption rate (OCR) was estimated with Seahorse Mito Stress Test Assay. Lactate production and glucose consumption were quantified using corresponding assay kits. Western blot was employed to analyze the expression of stem cell markers, glycolysis- and MEK/ERK/PD-L1 signaling pathway-related proteins. In vivo, tumor size and weight were recorded, and immunohistochemical staining was used to assess MEK/ERK/PD-L1 and KI67 expression in tumor tissues from nude mice.

Results It was observed that NCAPH expression is upregulated in ovarian cancer cells. Silencing NCAPH led to repression of both stemness characteristics and glucose metabolism reprogramming. Furthermore, knockdown of NCAPH inhibited the MEK/ERK/PD-L1 signaling pathway both in vitro and in vivo, resulting in suppressed tumor growth in mouse models.

Conclusion Collectively, silencing NCAPH impedes malignant progression of ovarian cancer through modulation of the MEK/ERK/PD-L1 pathway.

Clinical trial number Not applicable.

Keywords Ovarian cancer, NCAPH, MEK/ERK/PD-L1 pathway, Glucose metabolism reprogramming, Stemness

†Yingying Qi, Aiping Wang and Silin Chen contributed equally to this work.

*Correspondence:
Wei Chen
2624200814@qq.com
[1]Department of Gynecology, The Fifth Affiliated Hospital of Guangzhou Medical University, Guangzhou, China

Introduction

Ovarian cancer (OC) is recognized as a highly lethal malignancy among women, primarily due to its high rates of recurrence and the frequent development of resistance to chemotherapy in patients [1]. It has been reported that over 70% OC patients are diagnosed at an advanced stage, largely because early-stage symptoms are often atypical or vague [2]. Currently, treatment modalities for OC include tumor debulking surgery combined with platinum-taxane-based chemotherapy [3]. Despite the fact that many OC patients indeed achieve remission from standard treatment methods, cancer recurrence and chemotherapy resistance bring tremendous challenges for most patients suffering from OC [4]. Hence, it is imperative to seek for potential therapeutic therapies for the management of OC.

Non-SMC condensin I complex subunit H (NCAPH) belongs to the condensin I complex, which has been classified within a superfamily of proteins known as kleisins [5]. NCAPH has been well-documented to be an oncogene in a variety of cancers. For example, NCAPH expression has been disclosed to be upregulated in endometrial cancer, breast cancer, and prostate cancer tissues compared to normal tissues and NCAPH upregulation closely associated with the poor prognosis [6–8]. Furthermore, silencing NCAPH can inhibit stemness and glycolysis in colon adenocarcinoma cells [9]. Our previous study demonstrated that NCAPH expression is elevated in OC cells and that it promotes proliferation, migration, invasion, and epithelial-mesenchymal transition (EMT) in OC cells [10]. However, the role and underlying mechanism of NCAPH concerning glycolysis and cell stemness in OC have yet to be investigated.

The MEK/ERK signaling pathway has been implicated in playing a critical role in various human cancers, contributing to processes such as cell proliferation, survival, metabolism, and migration [11]. Previous studies have demonstrated that the activation of MEK/ERK pathway can promote cell proliferation and glycolysis in breast cancer [12]. Furthermore, the inhibition of Raf/MEK/ERK signaling by caudatin has been shown to suppress stemness and glycolysis in non-small cell lung cancer cells [13]. Intriguingly, Li et al. have established that NCAPH activates MEK/ERK signaling pathway in bladder cancer to promote cell proliferation and suppress cell apoptosis [14]. Moreover, according to KEGG pathway (https://www.kegg.jp/kegg/pathway.html), MEK/ERK pathway is capable of regulating PD-L1 expression. However, the mechanism by which NCAPH interacts with the MEK/ERK/PD-L1 signaling pathway in ovarian cancer remains unclear.

In summary, this study aims to investigate the role of NCAPH in cellular stemness and glycolysis within ovarian cancer and elucidate its relationship with the MEK/ERK signaling pathway; this may provide novel insights into therapeutic strategies for treating ovarian cancer.

Materials and methods

Cell culture and treatment

The ovarian surface epithelial cell line HOSEPiC (cat. no. MZ-7847) was obtained from Ningbo Mingzhou Biotechnology Co., Ltd., while human ovarian cancer cell lines including SKOV3 (cat.no. iCell-h195), OVCAR3 (cat. no. iCell-h168), A2780 (cat.no. iCell-h004) and CAOV3 (cat.no. iCell-h037) were supplied by iCell Bioscience Inc. (Shanghai, China). All cells were cultured in Dulbecco's modified Eagle's medium (DMEM; Gibco) supplemented with 10% fetal bovine serum (FBS; Thermo Fisher Scientific) and 1% penicillin-streptomycin (both from Sigma-Aldrich). The incubation conditions included 5% CO2 at a temperature of 37 °C. To investigate the mechanism by which NCAPH is associated with the MEK/ERK/PD-L1 signaling pathway, MEK/ERK agonist LM22B-10 was administered to SKOV3 cells at a concentration of 50 μmol/L for one hour [15].

Cell transfection

For transfection, short hairpin RNAs (sh-RNA) specific to NCAPH (sh-NCAPH-1/2, were designed as follows: sh-NCAPH-1:Forward (F) 5′-CUGCCAGCCACAAUG AAUATT-3′ and reverse (R) 5′-UAUUCAUUGUGGCU GGCAGTT-3′; sh-NCAPH-2:Forward (F) 5′-CCAGCA GGAGUAUUGACAUTT-3′ and reverse (R) 5′-AUGUC AAUACUCCUGCUGGTT-3′), along with a corresponding scrambled sequence serving as a negative control (sh-NC). These constructs were synthesized by GenePharma, Shanghai, China. A total of 100 nM recombinant sh-RNAs were introduced into SKOV3 cells using Lipofectamine 2000 reagent under standard conditions at a temperature of 37 °C for a duration of 48 h according to recommended protocols. Following this period, SKOV3 cells were harvested for subsequent experiments.

Reverse transcription-quantitative PCR (RT-qPCR)

Total RNA was extracted from the sample SKOV3 cells using TRIzol reagent (Biosharp) and then reverse transcribed into complementary DNA (cDNA) by means of a commercial RevertAid™ cDNA Synthesis kit (Bio-Rad) in light of standard protocol. Subsequently, template amplification was conducted employing SYBR Green PCR Master Mix (Takara, Toyobo, Japan) on the 7500 Fast Real-time PCR system according to the operating manual. The relative gene expression was determined with $2^{-\Delta\Delta Ct}$ method [16]. The following were the sequences of primers: NCAPH forward (F), 5'-AGACGCCAAGGAAA GATGGG-3' and reverse (R), 5'-GGAACACACGCTCT GAAGGA-3' or GAPDH forward (F), 5'-TGTGGGCAT CAATGGATTTGG-3' and reverse (R), 5'-ACACCATGT

ATTCCGGGTCAAT-3'.All experiments were performed in triplicate.

Western blot

Subcutaneous tumor tissues from nude mice were excised into 2 mm × 2 mm fragments and subsequently mixed with lysis buffer containing protease and phosphatase inhibitors (Beyotime, China). SKOV3 cells were lysed using RIPA lysis buffer (Solarbio) to obtain protein extracts. Total proteins were extracted with RIPA lysis buffer (Solarbio), followed by quantification of protein concentration using bicinchoninic acid (BCA) protein assay kits according to the standard protocol provided by Thermo Fisher Scientific Inc. After separation via 8% SDS-PAGE, the proteins were transferred onto PVDF membranes, which were blocked with 5% BSA for 2 h at room temperature. The membranes were then sequentially incubated overnight with primary antibodies targeting NCAPH (ab200659; 1:1000; Abcam), SOX2 (ab92494; 1:1000; Abcam), OCT4 (ab200834; 1:10000; Abcam), PKM2 (15822-1-AP; 1:1000; Proteintech), HK2 (ab209847; 1:1000; Abcam), LDHA (ab52488; 1:5000; Abcam), p-MEK (ab307509; 1:1000; Abcam), p-ERK (ab201015; 1:1000; Abcam), PD-L1 (28076-1-AP; 1:1000; Proteintech), MEK (11049-1-AP; 1:5000; Proteintech), ERK (ab184699; 1:10000; Abcam) or GAPDH (ab9485; 1:2500; Abcam) overnight at 4 ℃ and horseradish peroxidase (HRP)-conjugated secondary antibodies (ab6721; 1:2000; Abcam) at room temperature for 1 h. Finally, the protein bands were visualized using virtue of enhanced chemiluminescence (ECL) detection reagent (Shanghai Yeasen Biotechnology Co., Ltd. and the density of protein was assessed with ImageJ software (version 1.49, National Institutes of Health).All experiments were performed in triplicate.

Spheroid formation assay

SKOV3 cells that exposed to serum-free DMEM/F12 medium introduced with B27 supplement, 20 ng/mL EGF, and 20 ng/mL bFGF (ThermoFisher Scientific, USA) in 96-well ultra-low attachment dishes were injected into 200 μL serum-free medium for at least 7 days [17, 18]. With the application of a Leica DMI microscope, the number of spheres with the size bigger than 70 μm was observed.All experiments were performed in triplicate.

Seahorse glycolysis stress test assay

The measurement of extracellular acidification rate (ECAR) was estimated utilizing a Seahorse XFe96 Analyzer with Seahorse XF Glycolytic Rate Assay Kit (Agilent, cat#: 103344-100) according to the recommended specifications.All experiments were performed in triplicate.

Detection of ECAR and OCR

For the detection of ECAR and oxygen consumption rate (OCR), either the Seahorse XF cell Mito Stress Test Kit (Agilent, cat#: 103015-100) or Seahorse XF Glycolytic Rate Assay Kit (Agilent, cat#: 103344-100) was utilized according to manufacturer instructions for use with the Agilent Seahorse XFe96 Analyzer (Agilent, California, CA, USA). Briefly, SKOV3 cells were seeded into an XF-96 plate and cultured in a Seahorse XF DMEM medium containing 10 mM glucose, 1 mM sodium pyruvate, and 2 mM L-glutamine for one hour without CO2 exposure [19]. Subsequently, oligomycin (final concentration 1.5 μM), luoro-carbonyl cyanide phenylhydrazone (FCCP, final concentration 1.0 μM), and rotenone/antimycin A (each final concentration 1.0 μM) were injected into each well prior to evaluating ECAR and OCR. All experiments were performed in triplicate.

Detection of lactate production and glucose consumption

The production of lactate and the consumption of glucose were assessed using a glucose assay kit (cat. no. CBA086; Sigma) and a lactate assay kit (cat. no. K607; Biovision) following the manufacturer's instruction after 24 h of cultivation. All experiments were performed in triplicate.

Subcutaneous tumor experiment

Prior to model establishment, female nude mice (25 g, 8 weeks) that obtained from Changzhou Cavens Laboratory Animals Technology Co., Ltd. were acclimatized to the experimental conditions and randomly assigned into Control, sh-NC and sh-NCAPH groups ($n = 6$). Transfected SKOV3 cells (1×10^6) were subcutaneously injected into the right flank of the mice. Tumor size was recorded on days 7, 10, 13, 16, 19 and 21. For anesthetization, mice were forced to inhale 1–1.5% isoflurane mixed with oxygen for approximately 4–5 min. On day 21, euthanasia was performed via cervical dislocation to obtain xenografts which were subsequently weighed immediately upon collection. All mice had free access to food and were maintained under pathogen-free conditions throughout the study period. The animal experiments adhered to ethical guidelines as outlined by project license No. G2024-160 issued by the Ethics Committee of Guangzhou Medical University; The surgical interventions and postoperative care for the animal complied with the guidelines and policies established for rodent survival surgery provided by Guangzhou Medical University.

Immunohistochemistry staining

Immunohistochemistry staining was performed on xenograft specimens from mice. The specimens were fixed in 4% paraformaldehyde, followed by dehydration, hyalinization, and paraffin embedding.For

immunohistochemistry, Immunohistochemistry staining was performed on xenograft specimens from mice. The specimens were fixed in 4% paraformaldehyde, followed by dehydration, hyalinization, and paraffin embedding. After blocking with BSA, the sections were incubated overnight at 4 °C with primary antibody targeting KI67 (cat. no. #AF0198; 1:50, Affinity), MEK1(antibodies. No. #A96159; 1:100, Affinity), ERK1(antibodies. No. #A305114; 1:100, Affinity) and PD-L1(antibodies. No. #A248773; 1 μg/ml, Affinity). The sections were then incubated with a goat anti-rabbit IgG secondary antibody (cat. no. #S0001; 1:200, Affinity) at 37 °C for 1 h. Immunohistochemical images were captured using an optical microscope, and the Immuno-Reactive Score (IRS) was calculated. The IRS was determined by multiplying two scores: (1) the percentage of positive cells in five randomly selected high-magnification fields, scored as follows: 0-10% = 1, 10-50% = 2, 50-75% = 3, and 75-100% = 4; and (2) the staining intensity, scored as follows: no staining = 0, light yellow or weak staining = 1, moderate staining = 2, and strong staining = 3.

Statistical analysis

All experiments were independently replicated three times. The experimental data collected were analyzed using GraphPad Prism software (version 8.0) and are presented as mean ± standard deviation. One-way analysis of variance (ANOVA) followed by Tukey's post hoc test was utilized to compare multiple groups. A p-value less than 0.05 was considered statistically significant.

Results

NCAPH expression was upregulated in ovarian cancer cells

NCAPH expression was significantly upregulated in ovarian cancer cells. To elucidate the role of NCAPH in ovarian cancer, we initially measured its mRNA and protein levels using RT-qPCR and western blot. Compared with the HOSEpiC group, NCAPH expression was markedly elevated in ovarian cancer cell lines, particularly in SKOV3 cells; therefore, SKOV3 cell line was selected for subsequent experiments (Fig. 1A). To investigate the effects of NCAPH knockdown, sh-NCAPH was transfected into SKOV3 cells, and transfection efficiency was assessed by RT-qPCR and western blot. Compared with the sh-NC group, NCAPH expression was substantially reduced, especially in the sh-NCAPH-2 group; hence, sh-NCAPH-2 was chosen for further studies (Fig. 1B).

NCAPH silencing inhibited the stemness of ovarian cancer cells

To investigate the effect of NCAPH silencing on the stemness of ovarian cancer cells, we initially conducted a spheroid formation assay. Compared to the sh-NC group, the stemness of cells was significantly reduced

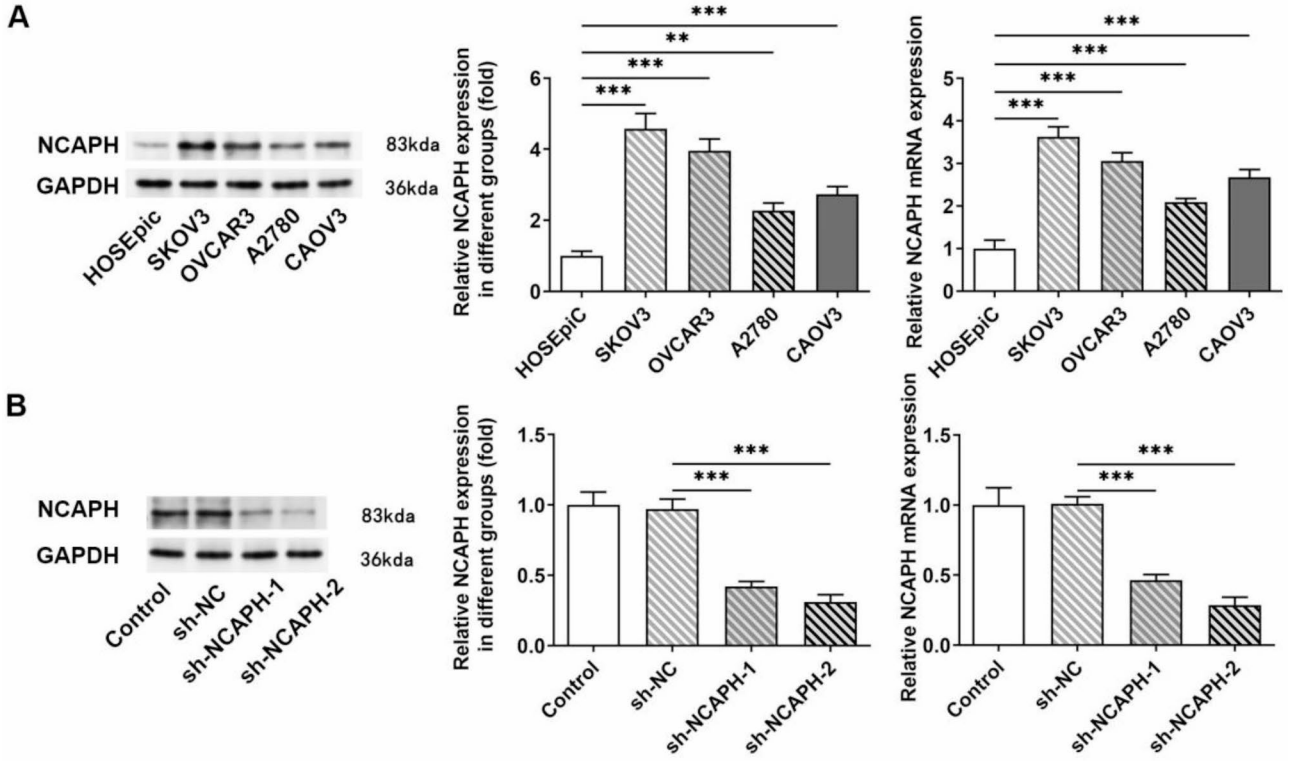

Fig. 1 NCAPH expression was upregulated in ovarian cancer cells. **A** The mRNA and protein expression of NCAPH were assessed using RT-qPCR and western blot analysis. **B** was validated by RT-qPCR and western blot analysis. All experiments were performed in triplicate.***$P < 0.001$

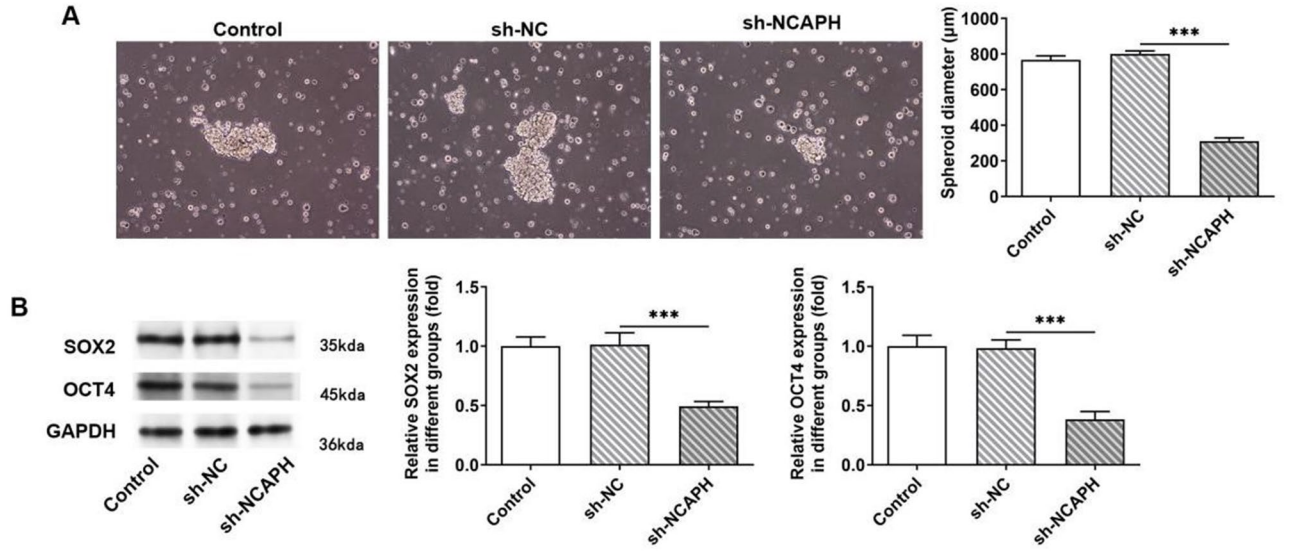

Fig. 2 NCAPH silencing inhibited the stemness of ovarian cancer cells. **A** Spheroid formation assays were conducted to evaluate cell stemness. **B** Western blot analysis was used to detect the expression levels of stem cell markers. All experiments were performed in triplicate.***$P < 0.001$

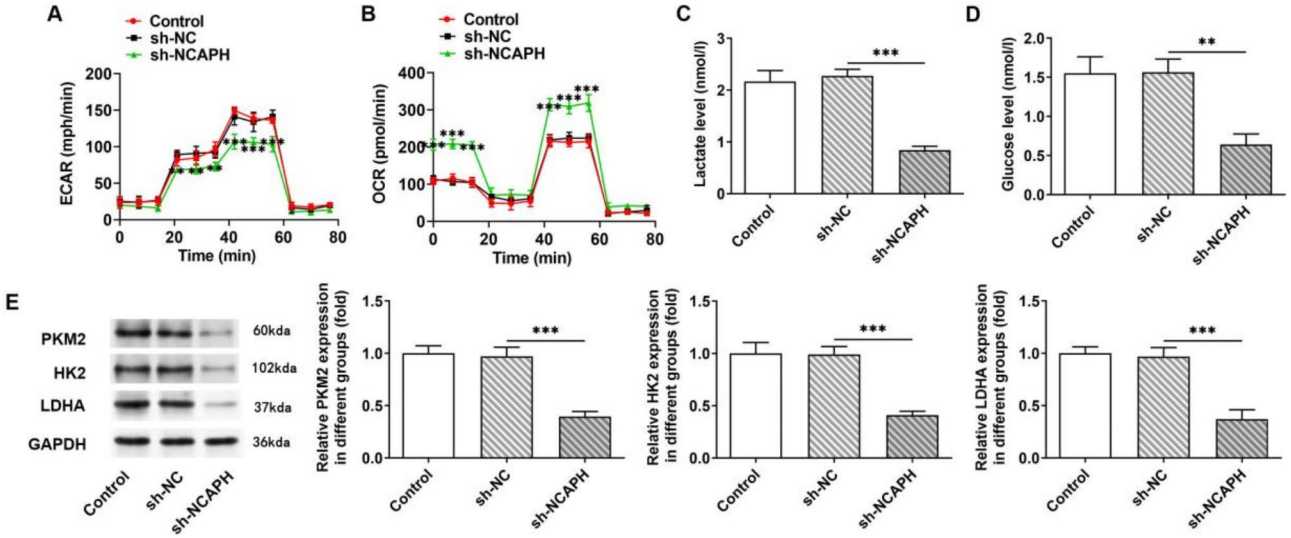

Fig. 3 NCAPH silencing inhibited glucose metabolism reprogramming in ovarian cancer cells. **A** The ECAR level was measured using the Seahorse XF Glycolytic Rate Assay Kit. **B** The OCR level was assessed using the Seahorse XF cell Mito Stress Test Kit. **C** Lactate production was quantified using lactate assay kit. **D** Glucose consumption was determined using glucose assay kit. **E** The expression levels of glycolysis-related proteins were analyzed by Western blot. All experiments were performed in triplicate.**$P < 0.01$ and ***$P < 0.001$

after transfection with sh-NCAPH (Fig. 2A). Western blot analysis showed that NCAPH knockdown markedly decreased the protein expression levels of SOX2 and OCT4 in SKOV3 cells by contrast with the sh-NC group (Fig. 2B).

NCAPH silencing inhibited glucose metabolism reprogramming in ovarian cancer cells

Compared with the sh-NC group, NCAPH knockdown significantly decreased the extracellular acidification rate (ECAR) and increased the oxygen consumption rate (OCR) in SKOV3 cells (Fig. 3A-B). Additionally, lactate production and glucose consumption were markedly reduced in SKOV3 cells following transfection with sh-NCAPH (Fig. 3C-D). Western blot analysis revealed that NCAPH knockdown led to a significant reduction in the protein expression of PKM2, HK2, and LDHA in SKOV3 cells compared to the sh-NC group (Fig. 3E).

NCAPH silencing inhibited the MEK/ERK/PD-L1 signaling pathway in ovarian cancer cells

The impact of NCAPH silencing on the expression levels of proteins involved in the MEK/ERK/PD-L1 signaling pathway was evaluated using Western blot analysis. As

shown in Fig. 4, compared to the sh-NC group, NCAPH deficiency significantly reduced the protein expression of p-MEK, p-ERK, and PD-L1 in SKOV3 cells, suggesting that NCAPH silencing effectively suppresses the MEK/ERK/PD-L1 signaling pathway in ovarian cancer cells.

NCAPH silencing suppressed the stemness of ovarian cancer cells via inhibition of MEK/ERK/PD-L1 signaling pathway

To investigate the mechanism by which NCAPH influences this pathway, we treated SKOV3 cells with the MEK/ERK agonist LM22B-10 and repeated the functional experiments. Compared to the sh-NC group, NCAPH interference significantly reduced cell stemness, an effect that was partially reversed by LM22B-10 treatment (Fig. 5A). Additionally, the decreased protein expression levels of SOX2 and OCT4 in NCAPH-silenced SKOV3 cells were restored following LM22B-10 treatment (Fig. 5B).

NCAPH silencing suppressed glucose metabolism reprogramming in ovarian cancer cells via inhibition of MEK/ERK/PD-L1 signaling pathway

Compared with the sh-NCAPH group, LM22B-10 treatment increased the ECAR level whereas decreased OCR level in SKOV3 cells (Fig. 6A-B). Additionally, the reduced lactate production and glucose consumption in NCAPH-silenced SKOV3 cells were partially restored by LM22B-10 treatment (Fig. 6C-D). Moreover, NCAPH interference markedly reduced the protein expression of PKM2, HK2 and LDHA in SKOV3 cells compared to the sh-NC group, whereas LM22B-10 treatment reversed these effects, as evidenced by increased expression of PKM2, HK2, and LDHA in the LM22B-10 + sh-NCAPH group (Fig. 6E).

NCAPH silencing suppressed tumor growth in mice

The appearance of mice and tumor were demonstrated in Fig. 7A. NCAPH interference markedly reduced both the tumor volume and weight (Fig. 7B-C). urthermore, western blot analysis revealed that silencing NCAPH led to decreased protein expression levels of p-MEK, p-ERK, and PD-L1 in tumor tissues of nude mice (Fig. 7D). Additionally, the IRS among the three groups indicated that, compared with the sh-NC group, the depletion of NCAPH resulted in reduced expression levels of MEK, ERK, PD-L1, and KI67 (Fig. 8).

Discussion

Currently, the treatment methods for ovarian cancer (OC) remain suboptimal; therefore, it is crucial to identify key genes as therapeutic targets. This study demonstrates that silencing NCAPH inhibits glucose metabolism reprogramming and cell stemness in OC by suppressing the MEK/ERK/PD-L1 signaling pathway. Additionally, our findings indicate that NCAPH silencing

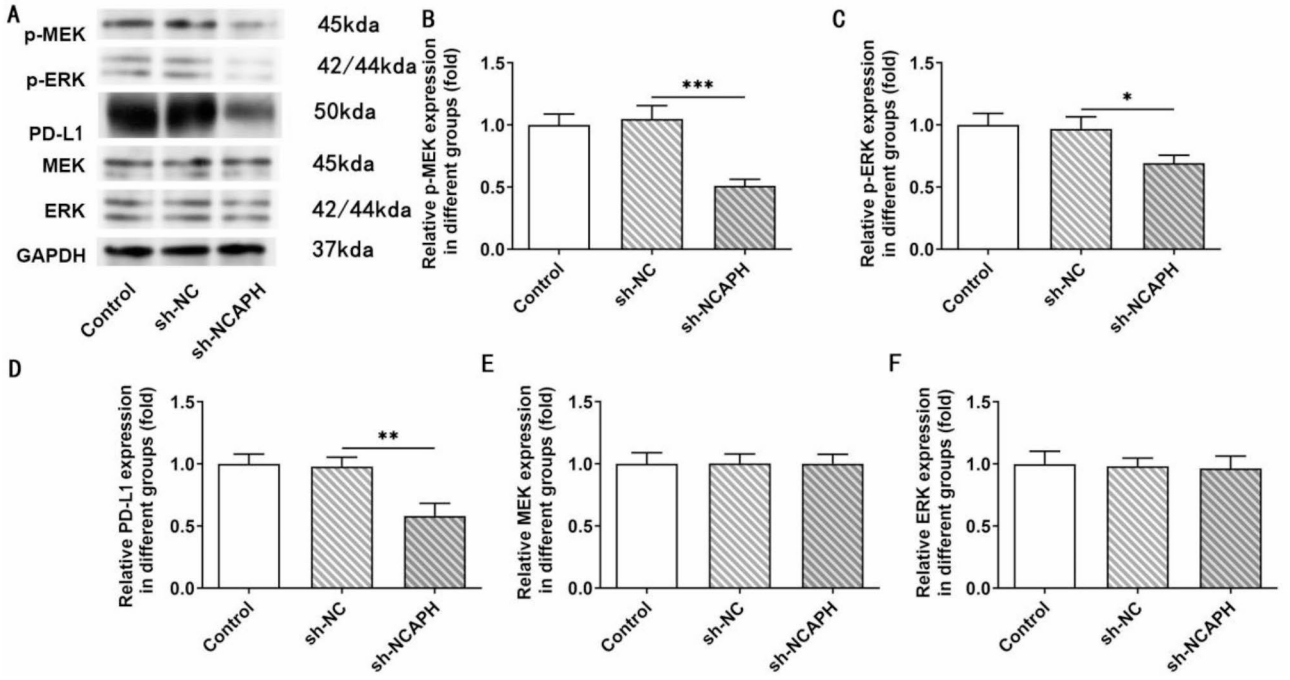

Fig. 4 NCAPH silencing inhibited the MEK/ERK/PD-L1 signaling pathway in ovarian cancer cells. **A** Western blot images showing the expression levels of p-MEK, p-ERK, PD-L1, MEK, ERK, and GAPDH in control, sh-NC, and sh-NCAPH groups. **B**-**F** Quantitative analysis of protein expression levels of p-MEK, p-ERK, PD-L1, MEK, and ERK by western blot in the three groups mentioned above. All experiments were performed in triplicate.*$P < 0.05$, **$P < 0.01$ and ***$P < 0.001$

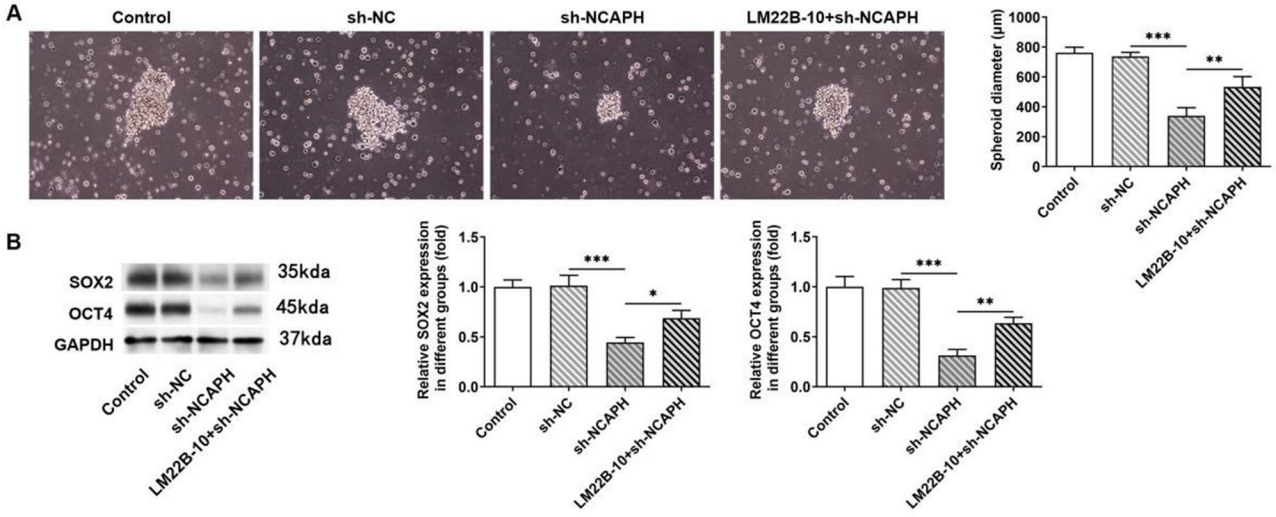

Fig. 5 NCAPH silencing suppressed the stemness of ovarian cancer cells via the inhibition of MEK/ERK/PD-L1 signaling pathway. **A** Cell stemness was assessed using a spheroid formation assay. **B** The expression levels of stem cell markers were evaluated using Western blot analysis. All experiments were performed in triplicate.*$P < 0.05$, **$P < 0.01$ and ***$P < 0.001$

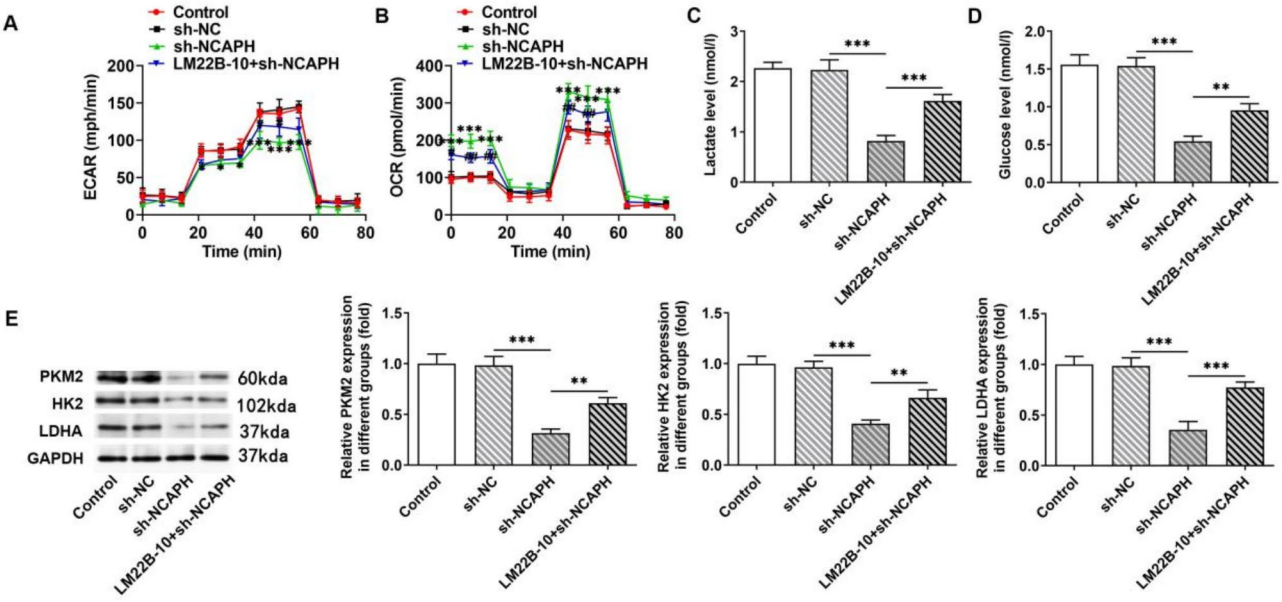

Fig. 6 NCAPH silencing suppressed glucose metabolism reprogramming in ovarian cancer cells. **A** The ECAR level was measured using the Seahorse XF Glycolytic Rate Assay Kit. **B** The OCR level was assessed using Seahorse XF cell Mito Stress Test Kit. **C** The lactate production was detected using lactate assay kit. **D** The glucose consumption was assessed using the glucose assay kit. **E** The expression of glycolysis-related proteins were evaluated by Western blot analysis. All experiments were performed in triplicate.*$P < 0.05$, **$P < 0.01$ and ***$P < 0.001$ vs. sh-NC, #$P < 0.05$ and ##$P < 0.01$ vs. sh-NCAPH

can suppress tumor growth in xenograft mouse models. These preliminary results suggest that NCAPH may serve as a promising therapeutic target for the treatment of OC.

NCAPH has been recognized as an oncogene in multiple types of cancers. For instance, in gastric cancer, NCAPH expression is significantly upregulated in both tissue samples and cell lines [20]. Additionally, Zhang et al. confirmed that NCAPH is highly expressed in human breast cancer cell lines [21]. Similarly, our study demonstrated a notable increase in NCAPH expression in ovarian cancer (OC) cell lines. Our previous research also established that NCAPH knockdown inhibits cell proliferation, migration, and epithelial-mesenchymal transition (EMT) in OC [10]. Consistent with these findings, Li et al. showed that NCAPH interference suppresses bladder cancer cell proliferation and markedly inhibits tumor growth in mice [14]. In line with this, the growth of xenograft tumors in mice was also suppressed by NCAPH silencing.

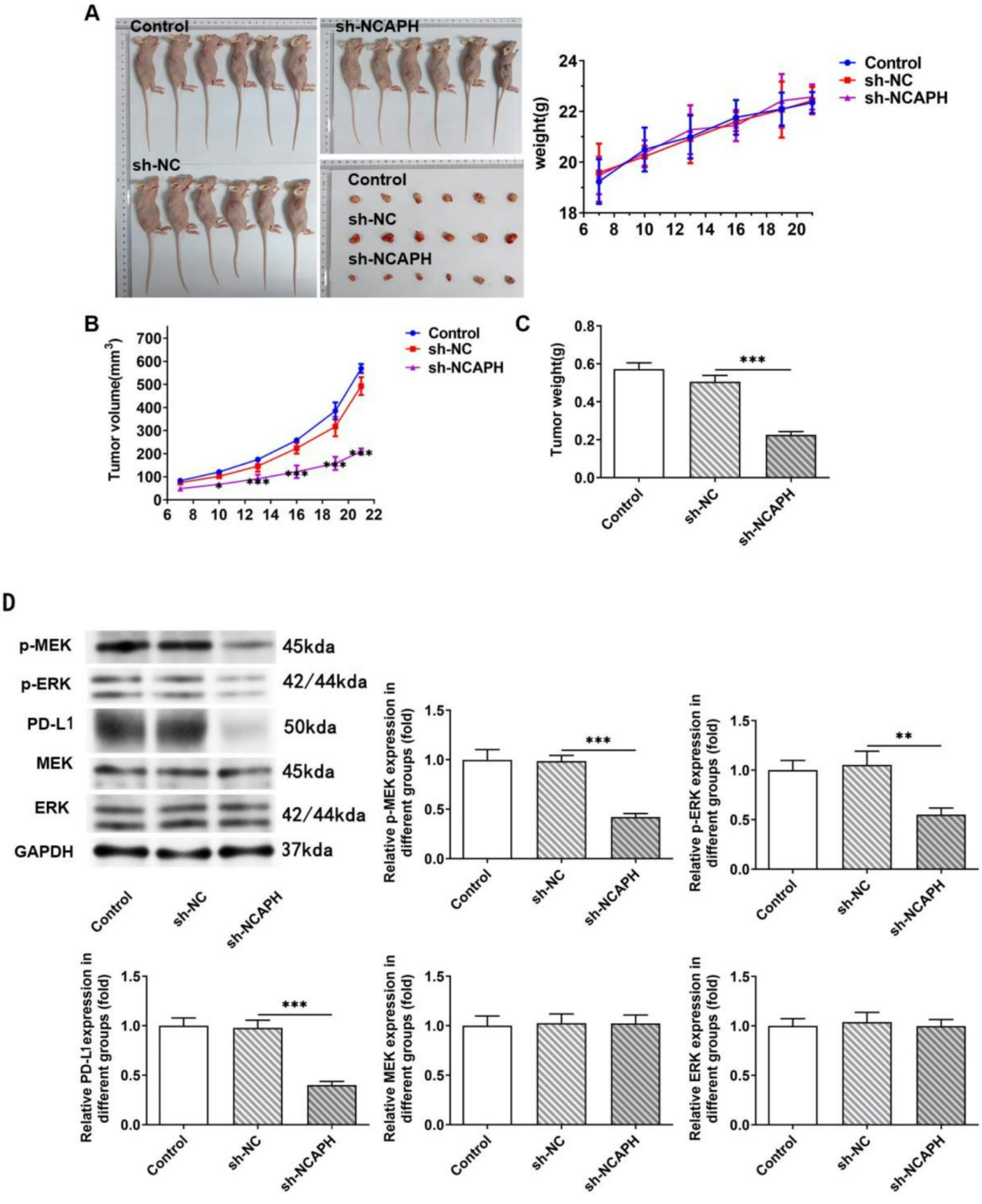

Fig. 7 NAPCH silencing suppressed tumor growth in mice. **A** The visual appearance of the mice and tumors. **B**-**C** The tumor volume and weight($n=6$ per group). **D** Expression levels of proteins related to the MEK/ERK/PD-L1 signaling pathway in subcutaneous tumor tissues from different groups were assessed using Western blot analysis. All experiments were performed in triplicate.*$P<0.05$, **$P<0.01$ and ***$P<0.001$

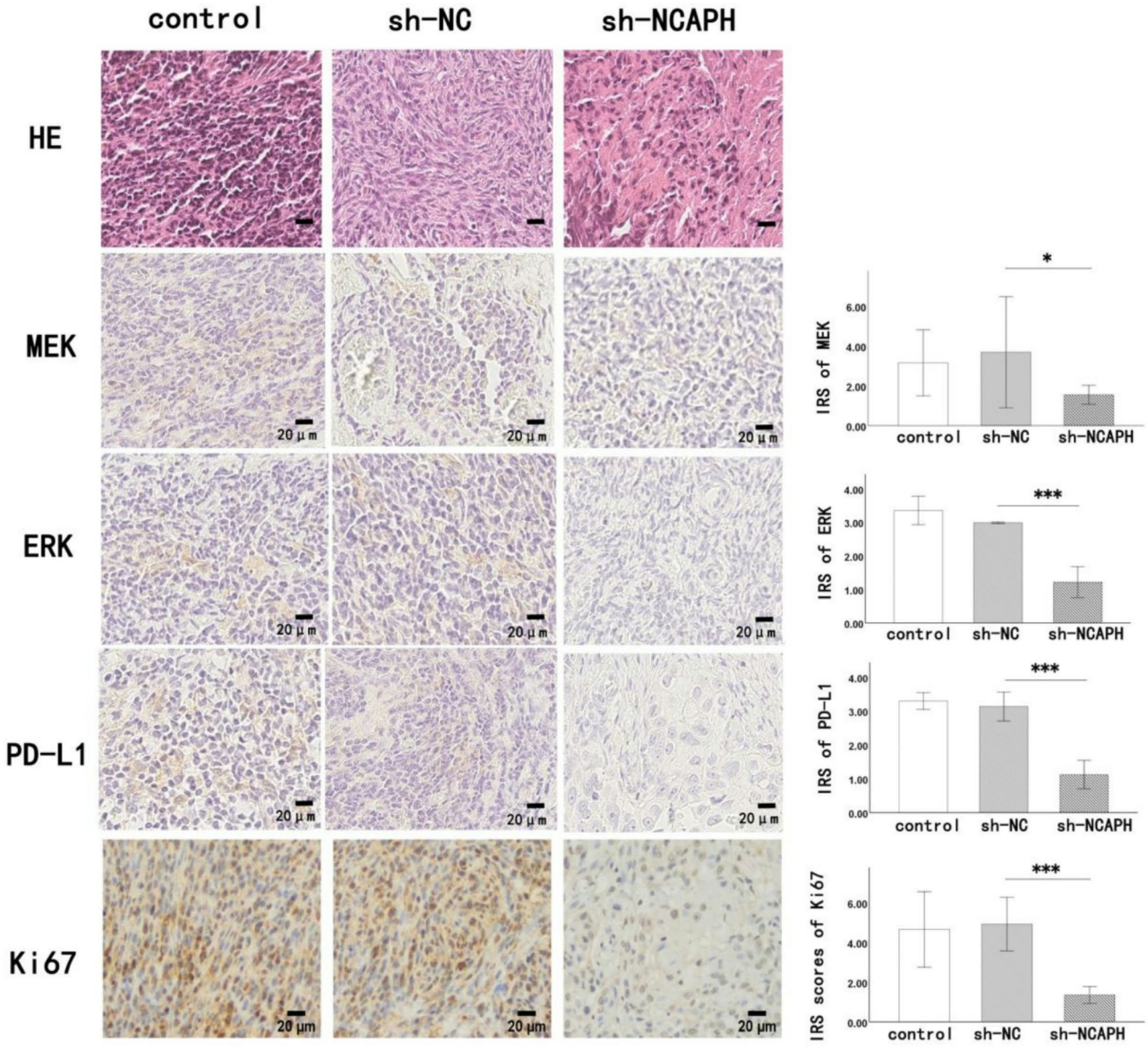

Fig. 8 The expression levels of MEK, ERK, PD-L1, and KI67 were assessed using hematoxylin and eosin (HE) staining and immunohistochemical staining. *$P < 0.05$, **$P < 0.01$ and ***$P < 0.001$

Cancer stem cells (CSCs), a subpopulation of cancer cells, possess self-renewal and differentiation capacities similar to those of normal stem cells, thereby promoting tumor growth and maintaining the heterogeneity of tumor mass [22, 23]. Consequently, CSCs are considered key contributors to tumor progression and advancement [24, 25]. Moreover, accumulating evidence indicates that CSCs play a critical role in chemotherapeutic resistance, leading to relapse and metastasis in ovarian cancer [26]. Therefore, targeting cell stemness may represent an effective therapeutic strategy for OC. Previous research has demonstrated that NCAPH upregulation enhances cell stemness in colon adenocarcinoma [9]. SOX2 is essential for maintaining stem cell pluripotency and forms a complex with OCT4 [27]. Overexpression of OCT4 is closely associated with tumorigenicity and metastasis [28]. Results of the present study indicate that interfering with NCAPH expression suppresses the stemness of OC cells, as evidenced by reduced protein levels of SOX2 and OCT4.

Cancer cells exhibit a distinct metabolic phenotype characterized by enhanced glycolysis, leading to increased lactate production [29]. Reprogramming of glucose metabolism is a well-established hallmark of cancer [30] and this metabolic shift facilitates the rapid proliferation of cancer cells [31]. Accumulating evidence has demonstrated that modulating glucose metabolism reprogramming can influence the progression of ovarian

cancer [32, 33]. ECAR reflects the flux of aerobic glycolysis, while OCR indicates mitochondrial oxidative respiration [34]. In this study, we observed that NCAPH silencing decreased ECAR levels while increasing OCR levels. Notably, circMYC knockdown in cervical cancer has been shown to suppress glycolysis, as evidenced by reduced lactate production and decreased glucose consumption [35]. NCAPH depletion in SKOV3 cells diminished lactate production and glucose consumption, suggesting that NCAPH depletion can inhibit glycolysis in OC.

As reported, inhibition of the MEK/ERK signaling pathway suppresses cell stemness and glycolysis in non-small cell lung cancer (NSCLC) and breast cancer [12, 13]. Moreover, KEGG pathway analysis indicates that the MEK/ERK pathway regulates PD-L1 expression. Accumulating evidence suggests that PD-L1 is positively correlated with immune system suppression and tumor progression. For example, overexpression of PD-L1 activates intracellular glycolysis via the mTOR signaling pathway, thereby promoting tumor growth and progression [36]. Additionally, Lei et al. have demonstrated that circ-HSP90A-mediated regulation of the PD-1/PD-L1 checkpoint accelerates cell growth, stemness, and immune evasion in NSCLC [37]. Furthermore, NCAPH has been shown to activate the MEK/ERK pathway in bladder cancer, thereby enhancing cell proliferation and inhibiting apoptosis [14]. In this study, we found that silencing NCAPH mediates the MEK/ERK/PD-L1 signaling pathway both in vitro and in vivo. Rescue experiments revealed that NCAPH deficiency inhibits cell stemness and glucose metabolism reprogramming in SKOV3 cells through the MEK/ERK/PD-L1 signaling pathway.

Although our study provides novel insights into the role of NCAPH in glucose metabolism reprogramming and cell stemness of ovarian cancer, its ability to promote ovarian cancer metabolism reprogramming and cell stemness via the MEK/ERK/PD-L1 pathway was only verified at the cellular and animal levels. The specific binding site between NCAPH and this pathway remains unexplored. Future studies will delve deeper into this topic to elucidate the precise mechanism by which NCAPH promotes metabolism reprogramming.

Conclusion

In conclusion, this study demonstrated that the silencing of NCAPH inhibits cell stemness and glucose metabolism reprogramming in SKOV3 cells, as well as suppresses tumor growth in xenograft mouse models. Mechanistically, NCAPH acts as a tumor promoter in ovarian cancer (OC) through the MEK/ERK/PD-L1 signaling pathway, suggesting that NCAPH may serve as a potential therapeutic target for OC.

Supplementary Information

The online version contains supplementary material available at https://doi.org/10.1186/s13048-025-01659-6.

Supplementary Material 1

Supplementary Material 2

Author contributions

QY and CW conceived and designed the project, QY and WA wrote the paper, CS acquired the data, QY analyzed and interpreted the data. All authors reviewed the manuscript.

Funding

This work was supported by the Science and Technology Projects in Guangzhou(2023A03J0821), the GuangDong Basic and Applied Basic Research Foundation-Joint fund (2021A1515220055).

Data availability

No datasets were generated or analysed during the current study.

Declarations

Competing interests

The authors declare no competing interests.

Received: 7 September 2024 / Accepted: 1 April 2025
Published online: 21 April 2025

References

1. Kielbik M, Przygodzka P, Szulc-Kielbik I, et al. Snail transcription factors as key regulators of chemoresistance, stemness and metastasis of ovarian cancer cells. Biochim Et Biophys Acta Reviews cancer. 2023;1878(6):189003.
2. Penny SM. Ovarian cancer: an overview. Radiol Technol. 2020;91(6):561–75. Epub 2020/07/02.
3. Sambasivan S. Epithelial ovarian cancer: review Article. Cancer Treat Res Commun. 2022;33:100629. Epub 2022/09/21.
4. Oronsky B, Ray CM, Spira AI et al. A brief review of the management of platinum-resistant-platinum-refractory ovarian cancer. Med Oncol. 2017;34(6):103. Epub 2017/04/27. https://doi.org/10.1007/s12032-017-0960-z. PubMed PMID: 28444622.
5. Sun C, Huang S, Wang H, Xie R, Zhang L, Zhou Q, et al. Non-SMC condensin I complex subunit H enhances proliferation, migration, and invasion of hepatocellular carcinoma. Mol Carcinog. 2019;58(12):2266–75.
6. Qiu X, Gao Z, Shao J, et al. NCAPH is upregulated in endometrial cancer and associated with poor clinicopathologic characteristics. Ann Hum Genet. 2020;84(6):437–46.
7. Lu H, Shi C, Wang S, Yang C, et al. Identification of NCAPH as a biomarker for prognosis of breast cancer. Mol Biol Rep. 2020;47(10):7831–42.
8. Cui F, Hu J, Xu Z, et al. Overexpression of NCAPH is upregulated and predicts a poor prognosis in prostate cancer. Oncol Lett. 2019;17(6):5768–76.
9. Lei Y, Wang D, Chen W, et al. FOXM1/NCAPH activates Glycolysis to promote colon adenocarcinoma stemness and 5-FU resistance. Anticancer Drugs. 2023;34(8):929–38.
10. Qi Y, Mo K, Zhang T. A transcription factor that promotes proliferation, migration, invasion, and epithelial-mesenchymal transition of ovarian cancer cells and its possible mechanisms. Biomed Eng Online. 2021;20(1):83. Epub 2021/08/18.
11. Xue J, Li Y, Yi J, et al. HAVCR1 affects the MEK/ERK pathway in gastric adenocarcinomas and influences tumor progression and patient outcome. Gastroenterol Res Pract. 2019;2019:6746970. Epub 2019/12/31.
12. Xu D, Xu N, Sun L, et al. TG2 as a novel breast cancer prognostic marker promotes cell proliferation and Glycolysis by activating the MEK/ERK/LDH pathway. BMC Cancer. 2022;22(1):1267. Epub 2022/12/06.
13. Hou J, Chen Q, Huang Y, et al. Caudatin blocks the proliferation, stemness and Glycolysis of non-small cell lung cancer cells through the Raf/MEK/ERK pathway. Pharm Biol. 2022;60(1):764–73. Epub 2022/04/08.

14. Li B, Xiao Q, Shan L, et al. NCAPH promotes cell proliferation and inhibits cell apoptosis of bladder cancer cells through MEK/ERK signaling pathway. Cell Cycle. 2022;21(4):427–38. Epub 2022/01/04.
15. Yang X, Zheng YT, Rong W. Sevoflurane induces apoptosis and inhibits the growth and motility of colon cancer in vitro and in vivo via inactivating Ras/Raf/MEK/ERK signaling. Life Sci. 2019;239:116916. Epub 2019/10/19.
16. Livak KJ, Schmittgen TD. Analysis of relative gene expression data using real-time quantitative PCR and the 2(-Delta delta C(T)) method. Methods. 2001;25(4):402–8. Epub 2002/02/16.
17. Ivanov DP, Parker TL, Walker DA, et al. Multiplexing spheroid volume, resazurin and acid phosphatase viability assays for high-throughput screening of tumour spheroids and stem cell neurospheres. PLoS ONE. 2014;9(8):e103817. Epub 2014/08/15.
18. Ni H, Qin H, Sun C, et al. MiR-375 reduces the stemness of gastric cancer cells through triggering ferroptosis. Stem Cell Res Ther. 2021;12(1):325. Epub 2021/06/07.
19. Keturakis V, Narauskaitė D, Balion Z, Gečys D et al. The effect of SARS-CoV-2 Spike protein RBD-Epitope on immunometabolic state and functional performance of cultured primary cardiomyocytes subjected to hypoxia and reoxygenation. Int J Mol Sci. 2023;24(23). Epub 2023/12/09.
20. Wang Y, Li JQ, Yang ZL, et al. NCAPH regulates gastric cancer progression through DNA damage response. Neoplasma. 2022;69(2):283–91. Epub 2021/12/29.
21. Zhang T, Li P, Guo W et al. NCAPH promotes proliferation as well as motility of breast cancer cells by activating the PI3K/AKT pathway. Physiology international. 2022. Epub 2022/09/07.
22. Beck B, Blanpain C. Unravelling cancer stem cell potential. Nat Rev Cancer. 2013;13(10):727–38.
23. Colak S, Medema JP. Cancer stem cells–important players in tumor therapy resistance. Febs J. 2014;281(21):4779–91.
24. Hu L, McArthur C, Jaffe RB. Ovarian cancer stem-like side-population cells are tumourigenic and chemoresistant. Br J Cancer. 2010;102(8):1276–83.
25. Zhang X, George J, Deb S, Degoutin JL, Takano EA, Fox SB, et al. The Hippo pathway transcriptional co-activator, YAP, is an ovarian cancer oncogene. Oncogene. 2011;30(25):2810–22.
26. Das PK, Islam F, Lam AK. The roles of cancer stem cells and therapy resistance in colorectal carcinoma. Cells. 2020;9(6). Epub 2020/06/07.
27. Zhang S, Cui W. Sox2, a key factor in the regulation of pluripotency and neural differentiation. World J Stem Cells. 2014;6(3):305–11.
28. Zeineddine D, Hammoud AA, Mortada M, Boeuf H. The Oct4 protein: more than a magic stemness marker. Am J Stem Cells. 2014;3(2):74–82.
29. Israelsen WJ, Vander Heiden MG. Pyruvate kinase: function, regulation and role in cancer. Semin Cell Dev Biol. 2015;43:43–51.
30. Ward PS, Thompson CB. Metabolic reprogramming: a cancer hallmark even Warburg did not anticipate. Cancer Cell. 2012;21(3):297–308.
31. Huang Y, Chen Z, Lu T, et al. HIF-1α switches the functionality of TGF-β signaling via changing the partners of Smads to drive glucose metabolic reprogramming in non-small cell lung cancer. J Exp Clin Cancer Res. 2021;40(1):398.
32. Chen Y, Liu L, Xia L, et al. TRPM7 Silencing modulates glucose metabolic reprogramming to inhibit the growth of ovarian cancer by enhancing AMPK activation to promote HIF-1α degradation. J Exp Clin Cancer Res. 2022;41(1):44.
33. Tan S, Yu H, Xu Y, et al. Hypoxia-induced PPFIA4 accelerates the progression of ovarian cancer through glucose metabolic reprogramming. Med Oncol. 2023;40(9):272.
34. Hu C, Liu T, Han C, et al. HPV E6/E7 promotes aerobic Glycolysis in cervical cancer by regulating IGF2BP2 to stabilize m(6)A-MYC expression. Int J Biol Sci. 2022;18(2):507–21. Epub 2022/01/11.
35. Wang Z, Chen Y, Wang W, et al. CircMYC promotes cell proliferation, metastasis, and Glycolysis in cervical cancer by up-regulating MET and sponging miR-577. Am J Transl Res. 2021;13(6):6043–54.
36. Chang CH, Qiu J, O'Sullivan D, et al. Metabolic competition in the tumor microenvironment is a driver of cancer progression. Cell. 2015;162(6):1229–41.
37. Lei J, Zhu J, Hui B, et al. Circ-HSP90A expedites cell growth, stemness, and immune evasion in non-small cell lung cancer by regulating STAT3 signaling and PD-1/PD-L1 checkpoint. Cancer Immunol Immunotherapy: CII. 2023;72(1):101–24.

Publisher's note